

Some solid state chemistry with holes: Anion–cation redox competition in solids*

Jean Rouxel

Collège de France, 11 Place Marcelin Berthelot, 75231 Paris Cedex 5, France and
Institut des Matériaux de Nantes, UMR 6502, 2 rue de la Houssinière, BP 32229, 44322 Nantes Cedex 3, France

The raising up of the sp anionic band when going from oxides to the less electronegative sulphides, selenides or tellurides facilitates redox anion–cation interactions involving the d levels of transition metal cations and the sp levels of anionic groups. Holes may appear at the top of this sp valence band. These holes allow to practice a nice soft chemistry of the redox type by neutralizing them with electrons. One can also stabilize particular structural types. Finally, one can recognize three domains among transition elements, (i) on the left part of the period table layered structures are observed which involve M^{4+} cations and (chalcogen) $^{2-}$ anions, (ii) then the formation of sets of metal–metal bonds is observed, the geometry of which depends on both the initial electronic population and the electronic transfer to the metal, (iii) on the right hand side the highest oxidation state of the metals are not active anymore and the holes at the top of the sp band are taken up by a catenation of the anions.

In solid state chemistry most of the time a central role is assigned to cations. We have progressively become accustomed to describing the structures in terms of polyhedra that are built by the anions around the cations and which may be isolated or share corners, edges or faces. There are good reasons for this particular attention paid to cations: transition metal cations bring magnetic properties, eventually optical properties, and most of the time conduction bands are built up from their d orbitals. The anions are regarded to play a more passive role without any fluctuation of charge on them. Sometimes they appear to simply build a framework in the interstices of which the distribution of cationic species represents the important issue. This way of thinking can be traced back to the immense development of the chemistry of oxides and fluorides for which a hard sphere model remains largely valid.

In terms of electronic energy the said situation corresponds to one in which the anionic s and p levels form a band whose upper edge is low-lying. Except for the highest oxidation states, the d levels will be above the sp anionic band and will lead, indeed, to very ionic states. On going from oxygen to sulphur, selenium and

tellurium, the top of the sp band is raised. Also on going from left to right along a period of transition elements, the d levels are lowered. Therefore with an appropriate metal/non metal combination, interactions can take place between sp band and d cations levels that can be populated at the expense of the former. It may result in complex situations in which the structure of the anionic entity itself can be modified.

Our attention was drawn to these d–sp redox interactions as early as 1975 when preparing $NbSe_3$ (refs 1, 2). It is a pseudo one-dimensional compound showing a structure built up from a stacking of $[NbSe_6]$ trigonal prisms on top of each other. One would expect to observe the following distribution of charges: $Nb^{4+}(Se_2)^2Se^{2-}$, with respect to $ZrSe_3$ for example. But things are more complicated. In $NbSe_3$ there are three types of chains characterized by three different values of the Se–Se distances in the chalcogen pair (Figure 1). Chain III presents a true Se–Se pair (2.37 Å). Niobium is there in the +IV oxidation state. The d^1 electronic configuration leads to a half filled d_{z^2} conduction band built up along the chain by the corresponding Nb orbitals. Chain I shows a slightly bigger Se–Se distance (2.48 Å) which corresponds to a higher charge on the anions and less than one electron in the conduction band. These two chains carry the two charge density waves^{3,4}. From the q vectors of the associated distortions it is possible to get the precise electronic population in the d_{z^2} bands ($q = 2k_F$). The third chain (2.91 Å) is insulating. This rather unusual situation made $NbSe_3$ a model C.D.W. system. In addition, the depinning of a C.D.W. was observed for the first time in $NbSe_3$ (ref. 5). With respect to this contribution it is also a good illustration of the d–sp redox interaction. Depending on its length, i.e. the population of its antibonding state, the Se–Se pair behaves as an electron reservoir and governs the electronic population of the adjacent metallic chain.

Nevertheless the most well-known effect of the d–sp redox interaction is the transition from layered dichalcogenides on the left part of the periodic table to pyrites and marcasites on the right part of it. Let us start from ZrS_2 for example. It has the CdI_2 structural type with layers of edge-sharing $[ZrS_6]$ octahedra (Figure 2). In between the sp valence band which is mostly anionic in character and the corresponding cationic levels

*Text of First C. N. R. Rao lecture given at the Indian Institute of Science, Bangalore on 18 February 1997.

that have been pushed up towards higher energies (Figure 3) one finds the classical splitting of 3-below-2 d levels ($t_{2g} - e_g$). The d^0 configuration of Zr^{4+} leads to semi-conducting properties. In the neighbouring column the layered structure of NbS_2 is built up from edge-sharing trigonal prisms and results in a 1-below-2-below-2

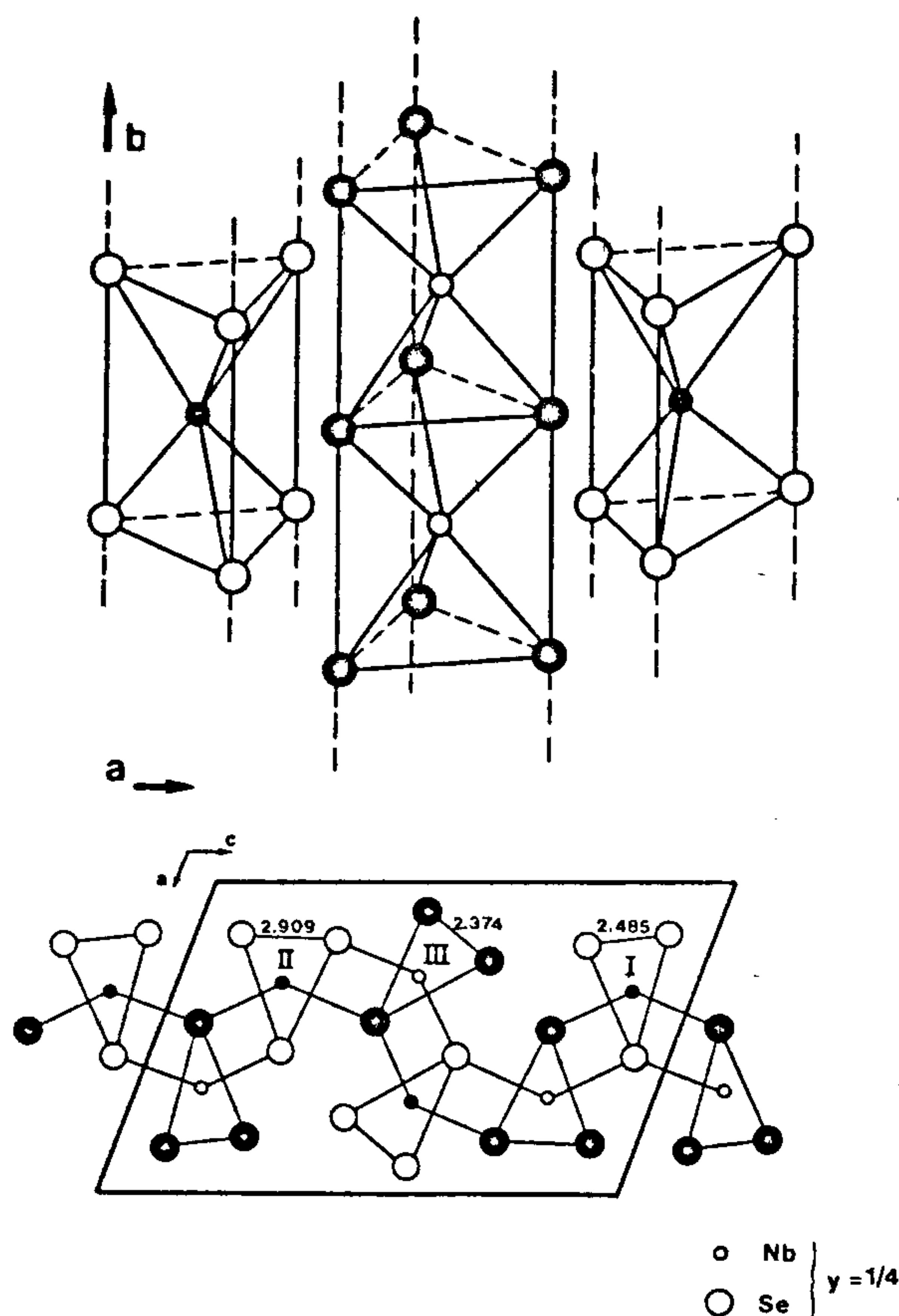


Figure 1. In the structure of $NbSe_3$, three types of chains running along the b direction correspond to three different values of the bond length in Se-Se 'pairs'.

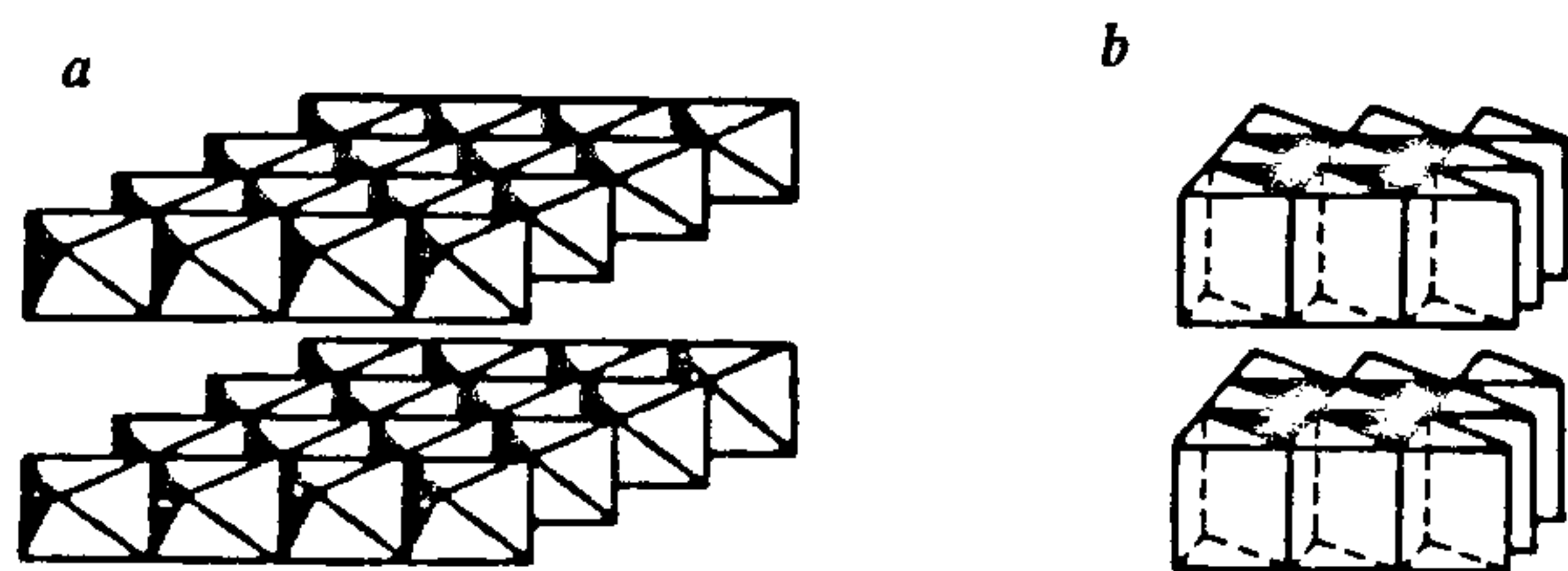


Figure 2. Layers of sharing edges octahedra (TiS_2 , ZrS_2) or trigonal prisms (NbS_2 , MoS_2) characterize the structures of dichalcogenides of the first transition elements in each row of the periodic table.

splitting of the d levels (a'_1, e', e''). The d^1 configuration of Nb^{4+} leads to a half filled a'_1 narrow band (essentially d_z in character), and metallic properties. Next to the right and with the same structure MoS_2 corresponds to a filled a'_1 band and semiconducting properties. Going further to the right one would expect to come back to the octahedral symmetry and a half filled t_{2g} band (the third d electron would destabilize the trigonal prismatic arrangement). But one observes now essentially pyrites or marcassites. MnS_2 for example is a pyrite. The reason is the following. On going to the right the d levels are progressively lower and, at a certain point, will enter the sp band. If empty d levels are in that situation, they will be filled at the expense of the sp band at the top of which holes will appear. The holes can remain isolated but usually the oxidation of the anions results in the formation of anionic pairs. This is the way one goes from layered TiS_2 with Ti^{4+} and $2S^{2-}$ to pyrites like FeS_2 with Fe^{2+} and a $(S_2)^{2-}$ pair^{6,7}.

The d-sp redox competition is not only the driving force for the above transition, but it is also active in both domains on each side of it. Some nice redox soft chemistry may also be done by playing with the holes at the top of a sp band. Neutralizing these holes may allow stabilizing structural types that would not exist otherwise. Finally the d-sp redox competition may generate domains with a different composition inside a given framework and results in structural intergrowths in highly covalent systems. We shall successively examine all these points.

Population of holes and anion-anion distances

With respect to the diagram of Figure 3c the chemist can play with the position of the top of a sp band and of the d levels. Playing with the top of the sp band just means that one will be comparing sulphides, selenides, tellurides of a given cation. The three titanium dichalcogenides, for example, have the same CdI_2 structure. With Ti^{4+} this would lead to an empty t_{2g} band and semi-conducting properties. TiS_2 is known indeed to be a semi-conductor but $TiSe_2$ is a semi-metal and $TiTe_2$ is a metal. The large decrease in electronegativity of the anion along this series results in a significant rise in the top of the sp band. The d levels are at first well detached above the sp band, than just skimming above it, or already inside the band⁸. In the last case ($TiTe_2$) we found from Mulliken overlap population calculations that 0.38 electrons have been transferred from tellurium to titanium. This transfer has important structural consequences. Because the top of the sp block, which has some antibonding character is being depopulated, the Te-Te distances are shortened. Short Te-Te contacts of 3.77 Å are observed; this is to be compared with the sum of the van der Waals radii which is 4.0 Å. Con-

versely, the existence of short anion–anion contacts in a given structure may be indicative of an electronic transfer to d cationic levels: this is of importance for the interpretation of magnetic and transport properties. We have already mentioned the particular case of NbSe_3 .

Now, instead of adjusting the top of the sp block, one can also lower (or raise) the position of the d levels by substituting a given metallic element with another one that is less (or more) electropositive. The d levels in HfTe_2 are higher in energy than those in TiTe_2 , and there is no electronic transfer from Te to Hf. Te–Te separation in HfTe_2 is consistent with the sum of the van der Waals radii. This trend in a column of the periodic table accounts for the stabilization of layered structures for the elements at the bottom while pyrites and marcasites are already appearing for the elements

at the top. MnS_2 is a pyrite but ReS_2 still has a layered structure.

The evolution of anion–anion distances as a function of the electronic population of antibonding states also occurs in the pyrite–marcasite domain. The interaction takes place between the e_g levels of the metal which are now low enough and the π^* levels of the $(\text{S}_2)^{2-}$ anion⁹. It results in a depopulation of the π^* anion levels and a shortening of the anion–anion distance along a series of pyrites like MnS_2 to CuS_2 and a reduction of the cation (copper is in the +1 oxidation state in CuS_2). In addition, the anion–anion interactions can go far beyond the formation of simple anionic pairs. As expected the effect is particularly enhanced in the case of tellurium. In CrTe_3 one can recognize $(\text{Te}_2)^{2-}$ pairs as well as $(\text{Te}_3)^{2-}$ trimers^{10,11}. In IrTe_2 (one can

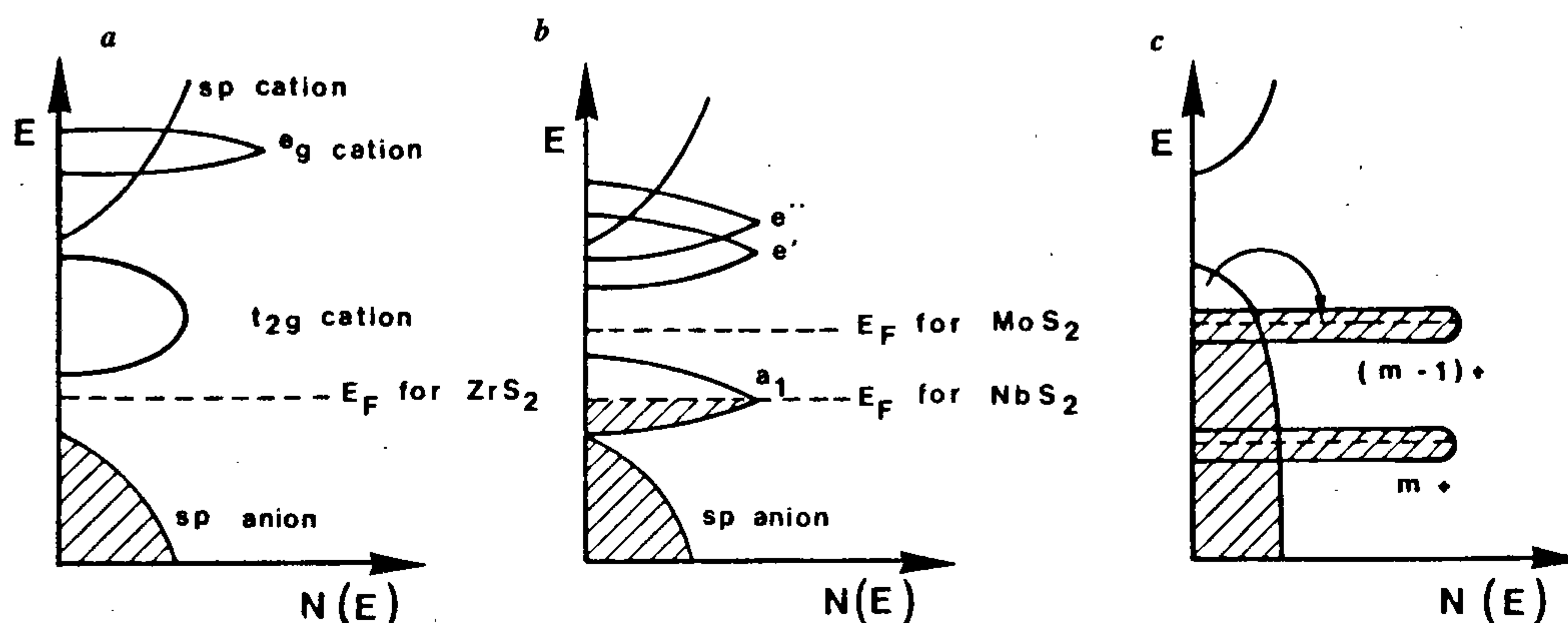


Figure 3. *a*, Band structure model for the 'octahedral' type; *b*, Trigonal prismatic type; *c*, Lowering of d levels and sp to d electron transfer on the right of the transition periods.

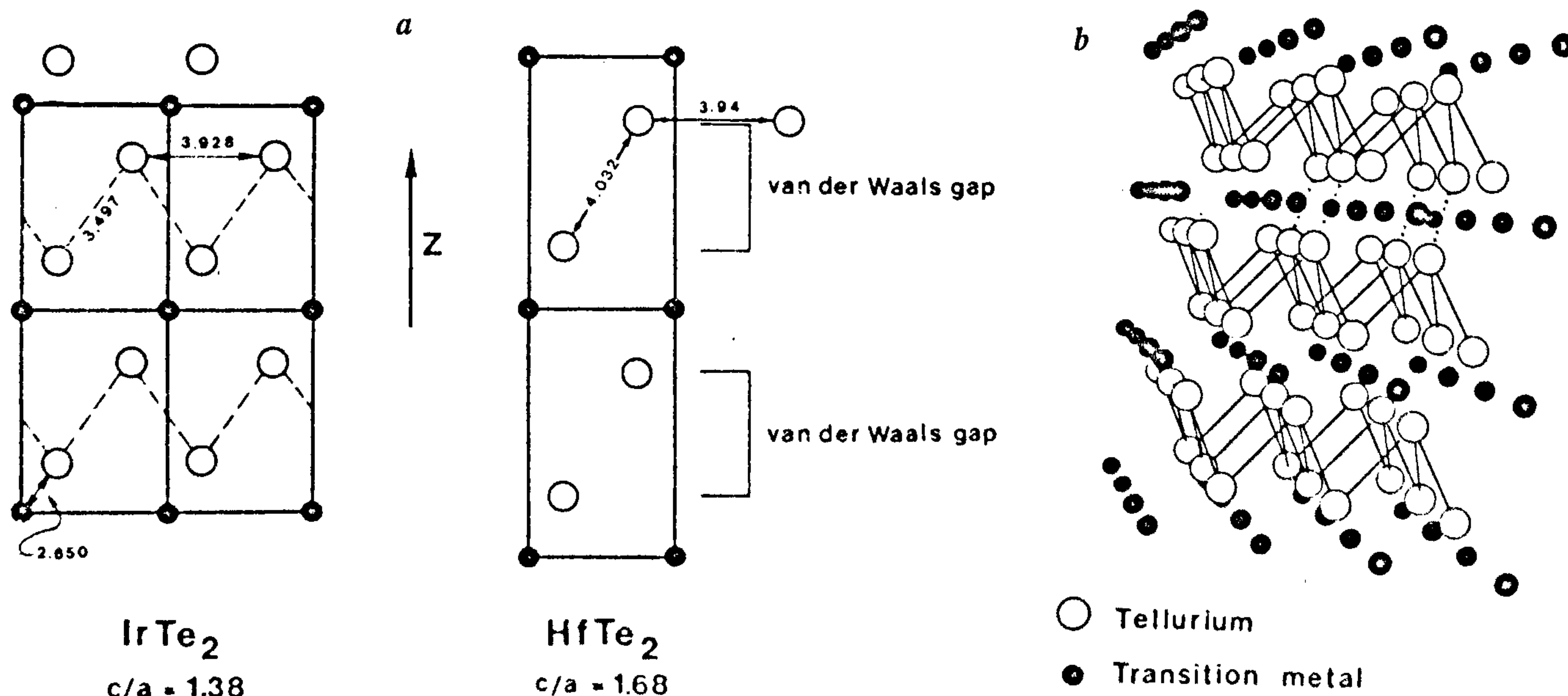


Figure 4. *a*, IrTe_2 structure compared to a true CdI_2 arrangement (HfTe_2); *b*, Perspective drawing of 3D IrTe_2 , showing the polymeric tellurium network.

conclude to) a full polymerization of the tellurium sublattice is attained with a distribution of long and short Te–Te distances. The transition metal is enclosed in pleated layers of polymeric tellurium (Figure 4). IrTe_2 represents a polymerized CdI_2 structural type.

In the course of these studies a quasi linear relationship appears between anion–anion distances and formal charges on them. Figure 5 shows the variation in the case of tellurides¹². It is precise enough to discuss composition and electron transfer in intercalation systems. For example, UTe_3 has a structure related to that of NbSe_3 although one finds only true Te–Te pairs therein ($d_{\text{Te-Te}} = 2.75 \text{ \AA}$), i.e. one has $\text{U}^{4+}\text{Te}^{2-}(\text{Te}_2)^{2-}$. Copper can be intercalated between the chains. A single crystal of $\text{Cu}_{0.36}\text{UTe}_3$ allowed a precise structural determination¹³. The Te–Te distance is increased in such a way that it fits perfectly with our curve considering a transfer of $0.36 e^-$ from copper to the Te–Te pair. This proves that copper is in the +1 oxidation state and that the electrons are totally taken up by Te–Te antibonding states which are the major constituents of the lowest unoccupied band. From a theoretical point of view it is not clear why such a perfect linear relationship is observed in the domain which has been studied. It is however important to remember that such a relation has also been pointed out by C. N. R. Rao in case of the oxides¹⁴.

Anion hole, and cation or anion clusterization

Regarding structural consequences of d–sp interactions, let us consider the ‘clusterization’ of metal atoms that may take place at sufficiently low temperatures in the slabs of layered chalcogenides. Indeed, on going from the titanium column to the neighbouring ones to the right of it in which the formal electronic configurations

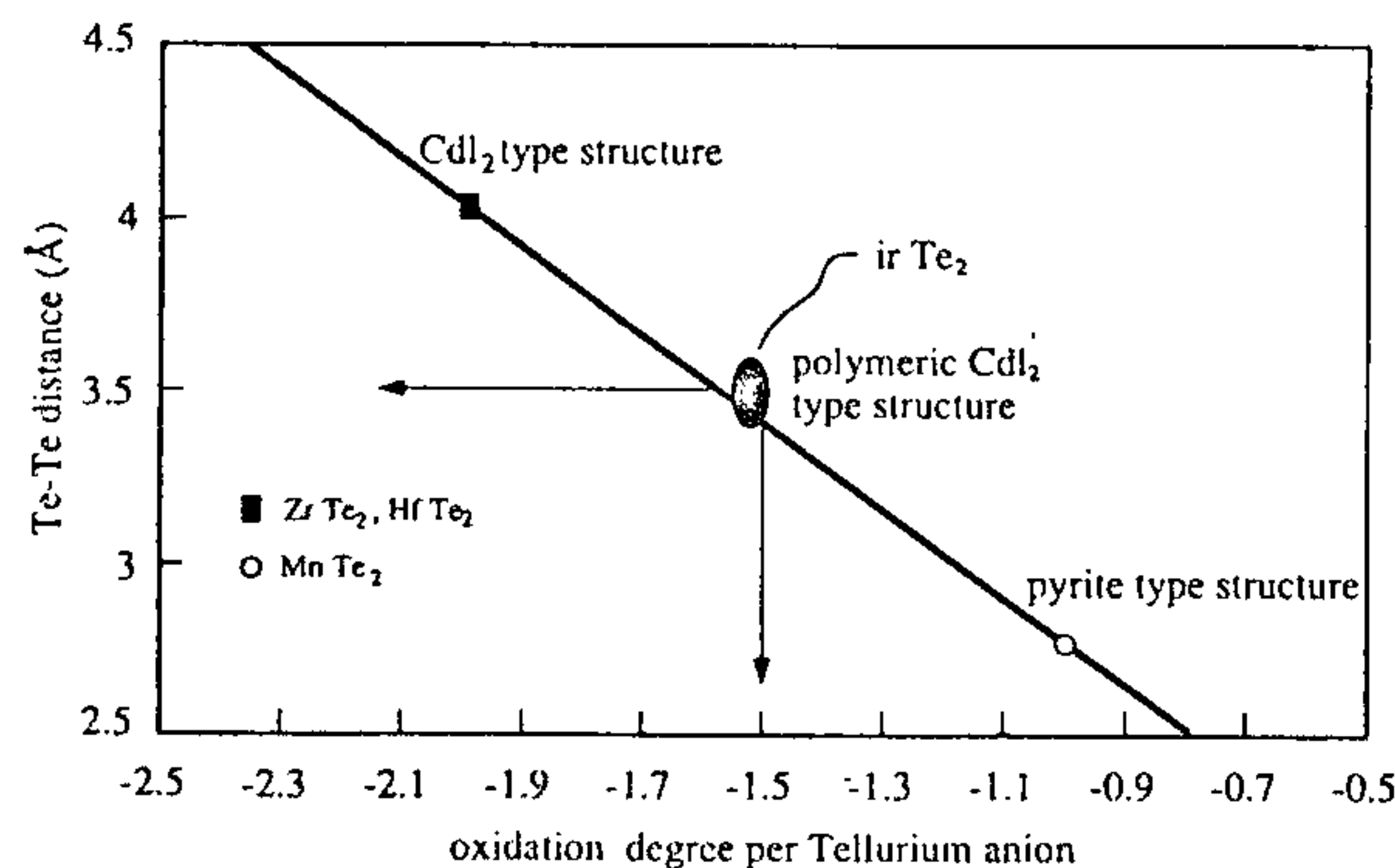


Figure 5. Variation in the Te–Te distance as a function of the formal oxidation state of tellurium (Te^{2-} in ZrTe_2 , $\text{Te}^{-1.5}$ in $\text{Ir}^{3+}(\text{Te}_2)$, Te^{-1} in MnTe_2).

for the metal are d^1 , d^2 and d^3 , it has been shown that these d electrons may be used in the formation of metal–metal bonds. Figure 6 shows typical sets of metal–metal bonds according to electron configuration. Interestingly the situation may differ for the tellurides as compared to sulphides. In VTe_2 there is an electron transfer of 0.25 electron from tellurium to vanadium⁸. The d^{1+x} electronic configuration of the metal results in a particular superlattice arrangement of V–V bonds that is different from the d^1 type and presages the d^2 situation. The electrons that originate from the top of the mostly anionic sp band and possesses π -antibonding character now take part in the formation of a net of metal–metal σ bonds.

The clusterization of the metal atoms through the setting of metal–metal σ bonds can be regarded as the symmetrical effect of the catenation of the anions through association of holes in the polymerized structures mentioned above.

Regarding the chemistry of transition metal chalcogenides, one can finally recognize three domains in the periodic table. On the left hand side low-dimensional structures with M^{4+} cations and Ch^{2-} anions are observed.

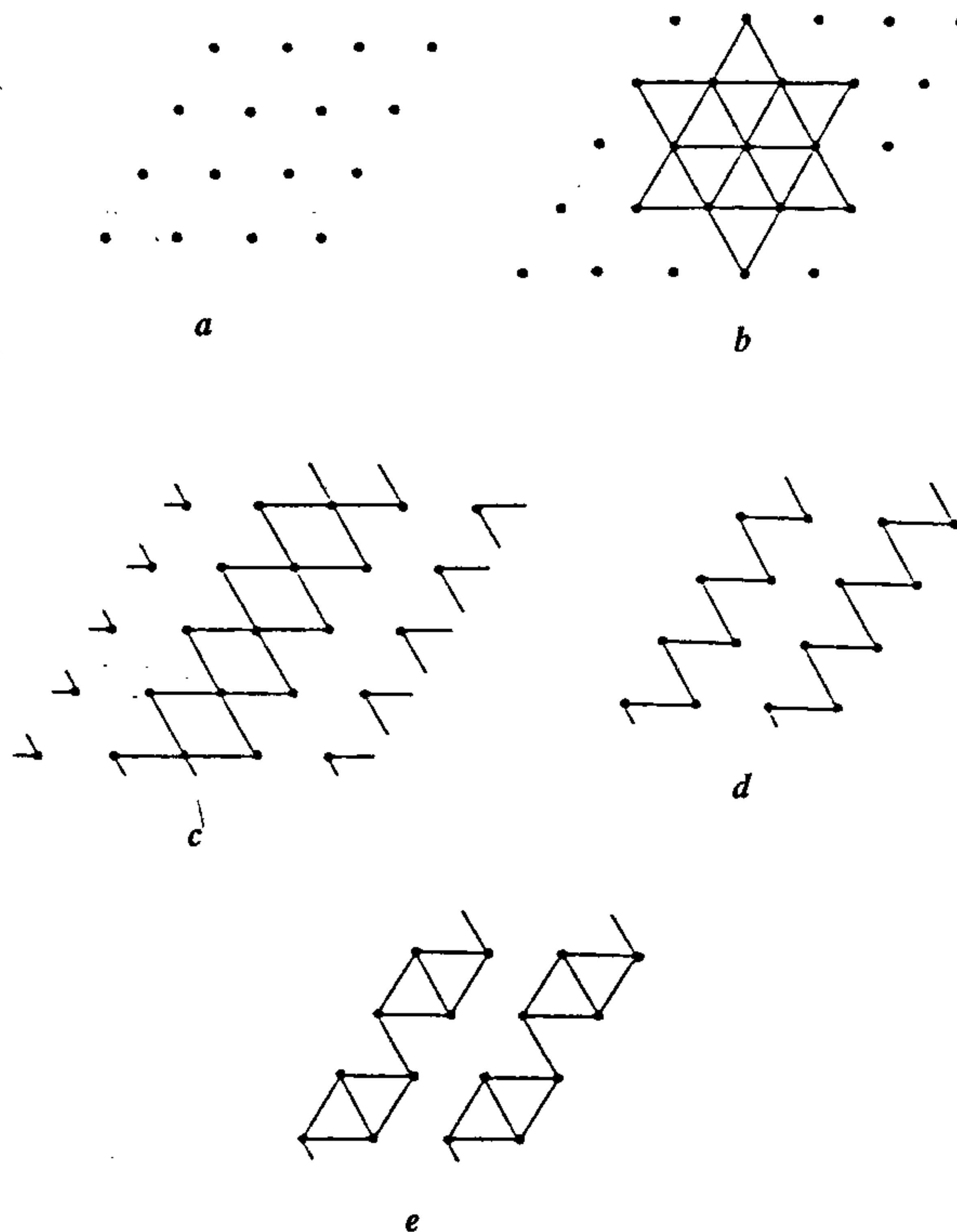


Figure 6. Cluster formation in the slabs of 2D chalcogenides: *a*, Undistorted hexagonal lattice typical for d^0 systems; *b*, Metal atom clustering for d^1 systems; *c*, Double zig-zag chain for d^2 ; *d*, Pattern in VTe_2 ; *e*, Metal–metal bonds in ReS_2 (d^3).

Then the destabilization of the highest oxidation states of transition metals results in the formation of sets of metal-metal bonds inside the slabs. The geometry of such arrangements depends on the initial electronic structure of the element as well as on the number of electrons that have been transferred from the sp chalcogen band. Finally, on the right part of the periods the high oxidation states are not active anymore. The holes at the top of the sp band are totally taken up by the anion under the form of a catenation which can go, through different steps, as far as a full polymerization of the anionic sublattice. The results can be transposed to phosphides, arsenides, bismuthides, iodides. The numerous solid phosphides with phosphorus associations can be discussed with the same approach¹⁵. Of course tellurides, with the highest sp band in the chalcogenide series represent the best example with the broadest developments. Figure 7 gives a classification of ditellurides according to the degree of association of the anions (or anionic polymerization AP). Starting from a true layered structure ($ZrTe_2$, $HfTe_2$), one can describe polymerizations along

the c parameter, i.e. in the stacking direction of the slabs either through slabs or through the van der Waals gap which separates slabs¹². One can also find polymerizations parallel to the a or/and b in plane parameters of the slabs. Starting from a true pyrite structure ($MnTe_2$) one describes also an association between $(Te_2)^{2-}$ pairs until a polymeric pyrite structure is obtained ($FeTe_2$, $RuTe_2$, ...). Any anion association through the van der Waals gap, $//c$, also gives rise to 3D networks although different from pyrite-marcasites arrangements.

Holes and redox chimie douce

In many systems, holes at the top of the sp band do not associate to form anionic pairs. Some nice chemistry may be done by playing with these holes. First of all the control of hole population at the top of the sp band can be illustrated by copper thiospinels. In $CuCr_2S_4$, polarized neutron studies as well as XPS measurements show the presence of one hole in the anionic sublattice which gives rise to p type conductivity and a strong

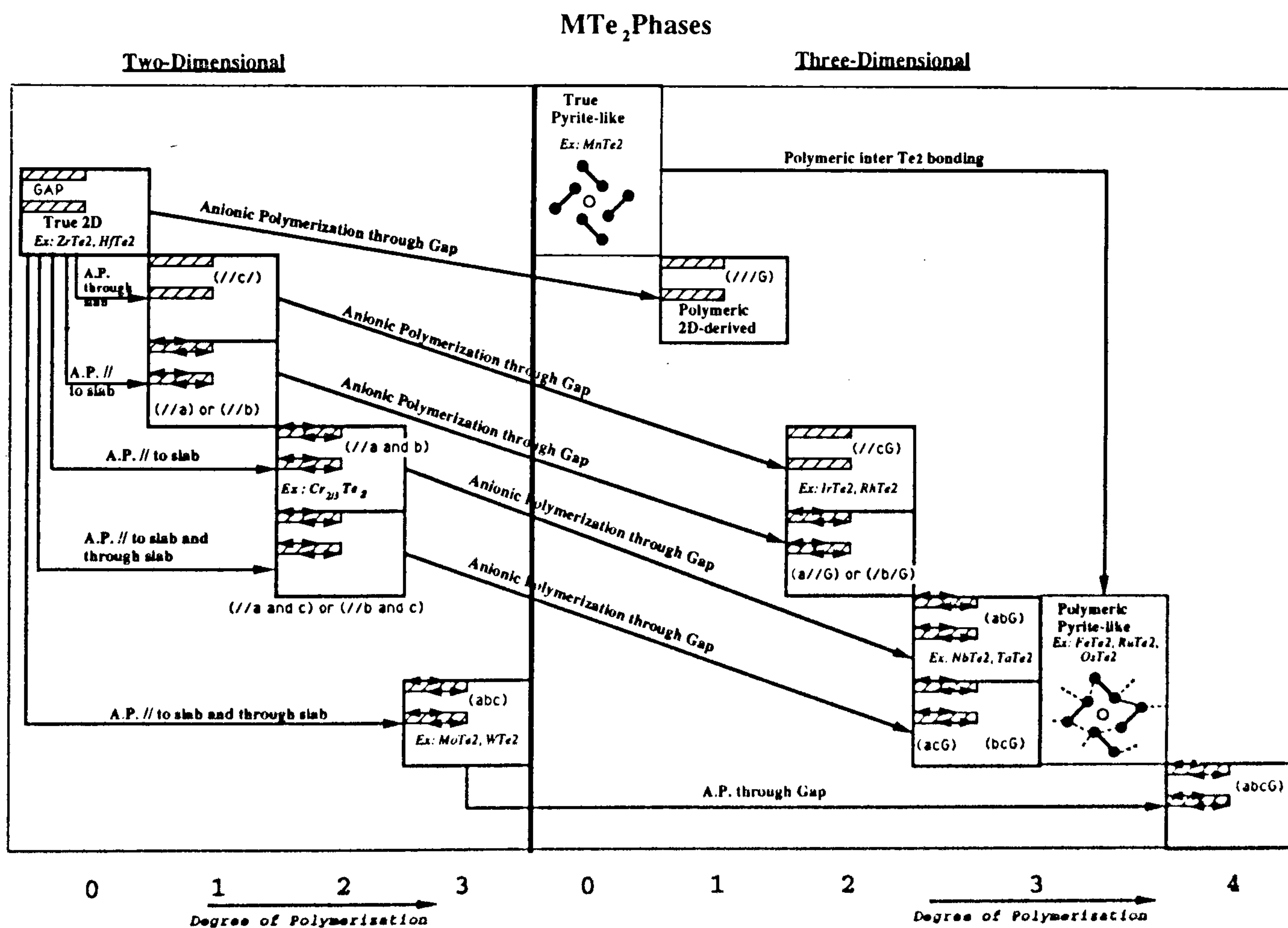


Figure 7. Classification of ditellurides according to dimensionality and 4 degrees of polymerization of tellurium (along the a direction, along a and b , intraslab, interslab). $ZrTe_2$ and $MnTe_2$ are chosen as true CdI_2 or pyrite-like structures from which all the evolutions can be described.

ferromagnetic coupling between Cr^{3+} cations¹⁶. Copper is in the +1 oxidation state as usual in sulphides: $\text{Cu}^+(\text{Cr}^{3+})_2(\text{S}^{2-})_3\text{S}^-$. The many empty sites of the spinel structure allow an additional intercalation of copper. Only one copper is intercalated, the associated electron neutralizing the hole. One gets $(\text{Cu}^+)_2(\text{Cr}^{3+})_2(\text{S}^{2-})_4$ which is a semi-conductor. More interesting is the fact that attempts to remove copper from CuCr_2S_4 have been unsuccessful. One could expect to get a layered CrS_2 of the CdCl_2 type with respect to the ABC stacking mode of sulphide anions in the spinel structure. The problem comes from the electron that has to be removed at the same time that Cu^+ ions are taken out. Either chromium or sulphide ions have to be oxidized. Chromium 4^+ is definitively unstable, the corresponding d level being too deeply engaged in the sp band. Creating another hole in the anionic sublattice does not seem to be possible, probably due to the too electronegative character of sulphur (see below). A third solution would have been an association of holes with a cut off of the top of the sp band to form an empty antibonding band. CrS_2 pyrite would then form. However a Jahn Teller distortion around Cr^{2+} cations is not acceptable for a very rigid pyrite structure.

NaCrS_2 is another candidate for deintercalation chemistry. With a αNaFeO_2 structure it would lead to a CdI_2 type of chromium disulphide. But this does not work either. However one can deintercalate Na from NaCrSe_2 and K from KCrSe_2 (ref. 17) and get a new layered CrSe_2 which can be formulated as $\text{Cr}^{3+}\text{Se}^{2-}\text{Se}^-$. Now there is one hole for two selenide ions. The highest level of the top of the sp band with respect to sulphides is certainly the explanation for this increased stability of holes.

Another way to succeed in deintercalation chemistry is to move to the left of the periodic table in order to have d levels at a higher energy and to play with the oxidation state of the cation. CuCr_2S_4 is an anionic mixed valence system, but CuTi_2S_4 is a cationic mixed valence system $\text{Cu}^{3+}\text{Ti}^{3+}\text{Ti}^{4+}(\text{S}^{2-})_4$. Deintercalating copper is possible and simply results in the oxidation of Ti^{3+} to Ti^{4+} . So-called cubic TiS_2 was formed which has the CdCl_2 structural type^{18,19}. The difference between the 'chimie douce' of NaCrSe_2 and CuCr_2S_4 (or similarly NaCrS_2) was the position of the top of the sp band. The difference between the 'chimie douce' of CuCr_2S_4 and CuTi_2S_4 is the position of the cationic d levels. In both cases CuTi_2S_4 and KCrSe_2 deintercalation is possible because a higher oxidation state can be reached by the metal (TiS_2 case) or because holes on the anion can be stabilized (CrSe_2 case).

Many other examples could be brought into discussion. They all refer to the same concepts. Let us consider only two of them. The first one represents a very spectacular case while the latter implies two redox mechanisms.

- (i) In thallium-copper sulphides and selenides, one finds a series of phases²⁰ which can be described in terms of interweaving TlCu_2X_2 slabs and more copper-rich slabs²⁰. Semi-conducting phases like TlCu_3Se_2 allow the removal of one copper from copper-rich slabs²¹. This can be achieved simply by using an aqueous ammonia solution which yields immediately the blue colour of copper tetramine cation $\text{Cu}(\text{NH}_3)_4^+$. One obtains TlCu_2Se_2 which presents one hole in the anionic sublattice, i.e. $\text{Tl}^+(\text{Cu}^+)_2\text{Se}^{2-}\text{Se}^-$. TlCu_2S_2 is obtained similarly from TlCu_3S_2 (ref. 22). In this case, chimie douce is the only route to obtain the phase with one hole in the sulphide layers. It illustrates once more the difference in stability for holes at the top of sulphide or selenide sp bands.
- (ii) Starting from Li_2FeS_2 one can deintercalate lithium in two steps. There is at first an oxidation of Fe^{2+} to Fe^{3+} followed by the formation of anionic pairs. Both the cations and anions are successively oxidized. One gets a new FeS_2 which is $\text{Fe}^{3+}(\text{S}_2^{2-})_{1/2}\text{S}^{2-}$. It is probably related to the IrS_2 structural type although the poor crystallinity of the samples did not allow a direct structural determination. The above information was obtained by Mössbauer studies as well as IR and Raman spectroscopies²³.

The latter example shows that one has to be cautious when interpreting any deintercalation process. It is of importance to carefully check the resulting structure. The starting structure does not necessarily behave as a rigid framework. Depending on the relative position of the d and sp bands, anionic association can occur and the oxidation of the cation may result in a changing of site.

The d-sp redox competition may have drastic consequences regarding the stoichiometries of a given series of compounds belonging to the same crystal structure. Let us consider the MPS_3 series of phases where M is an element of the first transition row. These have a layered structure: M^{2+} cation and P-P pairs occupy respectively 2/3 and 1/3 of the octahedral sites of TiS_2 like slabs $(\text{M}_{2/3}(\text{P}_2)_{1/3}\text{S}_2)$. On the right part of the periodic table NiPS_3 is easy to prepare and perfectly stoichiometric. However close to it, FePS_3 is difficult to reproduce with exactly the same stoichiometry. Vacancies occur in the iron sublattice. Ni^{2+} is perfectly stable and Ni^{3+} non stable in the presence of sulphur. In case of iron the corresponding d level is just moving above the sp band and Fe^{3+} can be stable depending on the sulphur pressure while preparing the samples. These ions have to be compensated by vacancies. MnPS_3 is a particular case due to the very high stability of Mn^{2+} , d^5 high spin in octahedral holes. But VPS_3 is in fact $\text{V}_{0.78}\text{PS}_3$ which is

a mixed valence $V^{2+}-V^{3+}$ compound²⁴. In case of titanium one even gets $Ti_{0.5}^{4+}PS_3$ (ref. 25).

Finally, it should be mentioned that an appropriate substitution in the cationic sublattice may allow sulphur p-band holes to be generated, which induce p-type conductivity. A good example of this is β - $BaCu_2S_2$ (ref. 26). It shows a two-dimensional structure with $[Cu_2S_2]^{2-}$ anionic slabs separated by Ba^{2+} layers (ThCr₂Si₂ type). The preparation of the substituted phase $K_xBa_{1-x}Cu_2S_2$ (ref. 27) leads to p-type conductivity. The compensation of charge cannot be achieved through an oxidation of some of the Cu^+ ions to Cu^{2+} . It is therefore taken up by the anionic sublattice and can be expressed by the formulation $(K^+)_x(Ba^{2+})_{1-x}(Cu^+)_2(S^{2-})_{2-x}(S^{-\cdot})_x$. One hole is introduced at the top of the sp band for each potassium, which allows an interesting variation in the physical properties.

Neutralization of holes and the stabilization of unusual structural types

A layered CrS_2 does not exist for the reasons discussed above. But there are compounds which show CrS_2 layers of the TiS_2 type. This is well illustrated by $NaCrS_2$ with a $\alpha NaFeO_2$ structure like $NaTiS_2$, the intercalation compound of Na in TiS_2 . One can formally consider that $NaCrS_2$ is the intercalation compound of Na in an hypothetical CrS_2 . Sodium has stabilized CrS_2 layers. Chromium is in the 3+ oxidation state, stable in the presence of sulphur. One can consider that the stabilization of the structure is achieved through the transfer of the electron associated with sodium which fills up the top of the sp band and prevents instabilities linked to the too low energy level of holes in sulphides or their possible association. If this interpretation is correct, it should be possible to stabilize CrS_2 slabs by other electron donors. It is indeed the case for $Si_{0.25}CrS_2$ (or $P_{0.20}VS_2$). Si or P are seated in tetrahedral holes at the surface of CrS_2 or VS_2 slabs²⁸. Their amount is such that the holes at the top of the sp band are exactly neutralized.

Many compounds could certainly be prepared on the basis of these ideas. Let us introduce only two series which show particular features regarding structures and chemical bonds and contribute to broaden the model. It is known that $NbTe_2$ layers similar to the NbS_2 or $NbSe_2$ ones are not stable by themselves. However, adding some silicon or germanium it was possible to stabilize such trigonal prismatic $NbTe_2$ layers in Ge_xNbTe_2 phases²⁹. But Si or Ge atoms are not simply seated in tetrahedral holes at the surface of the $NbTe_2$ slabs as has been found above. They occupy a rather unusual coordination in the middle of rectangular faces shared by two $[Te_6]$ trigonal prisms that are not centered by a niobium atom. Then, some of the Nb atoms are linked

together to form metal-metal pairs through a common triangular face between their adjacent trigonal prisms. Other Nb atoms remain isolated and build ribbons which mark out the regions in which M-M bonds are formed. The sequence according to which these regions alternate as a function of Ge (Si) concentration is responsible for the commensurate or incommensurate modulation of the structures (x rational or irrational). Figure 8 shows the building blocks that are used to construct a slab. There are three different ribbons. Ribbons a and b contain both Ge atoms and Nb-Nb pairs (with symmetrical positions); ribbon c contains only isolated Nb atoms. Variable numbers of pairs of ribbons a and b separate ribbon c and lead to a general formulation $NbGe(1 + n/3 + 2n)Te_2$. With an infinite succession of ribbons a and b, and no c ribbon, one gets the end member $NbGe_{1/2}Te_2$. Ge is in the +2 oxidation state as shown by an analysis of the density of states curves which reveals the presence of levels with Ge 4s character lying about 4 eV below the Fermi level, while the Ge 4p levels are well above E_f . Two electrons have been used to reduce niobium atoms and one could associate them with the formation of Nb-Nb pairs because the number of these pairs is exactly equal to the number of Ge atoms ($NbGe_{1/2}Te_2$ without c ribbons is a clear illustration of that). But things are generally more complicated because all Nb atoms have been reduced. Electrons are also coming from the top of the sp band. Indeed the partial depopulation of these anionic states with antibonding character results in a $[Te_4]$ catenation. Two Te in one slab are associated with two in an adjacent one, through the van der Waals gap. Successive slabs are thus fixed relative to each other. In all com-

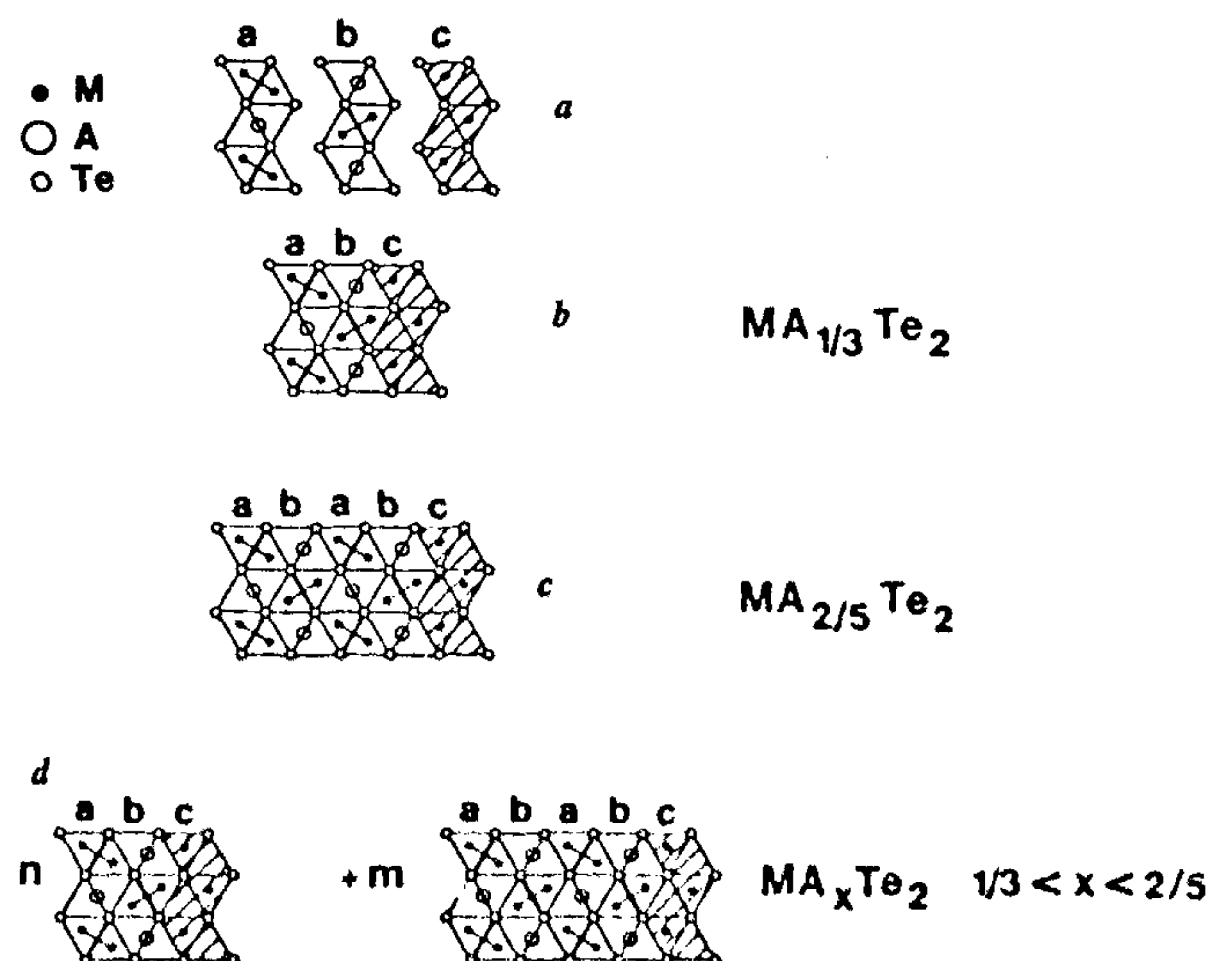
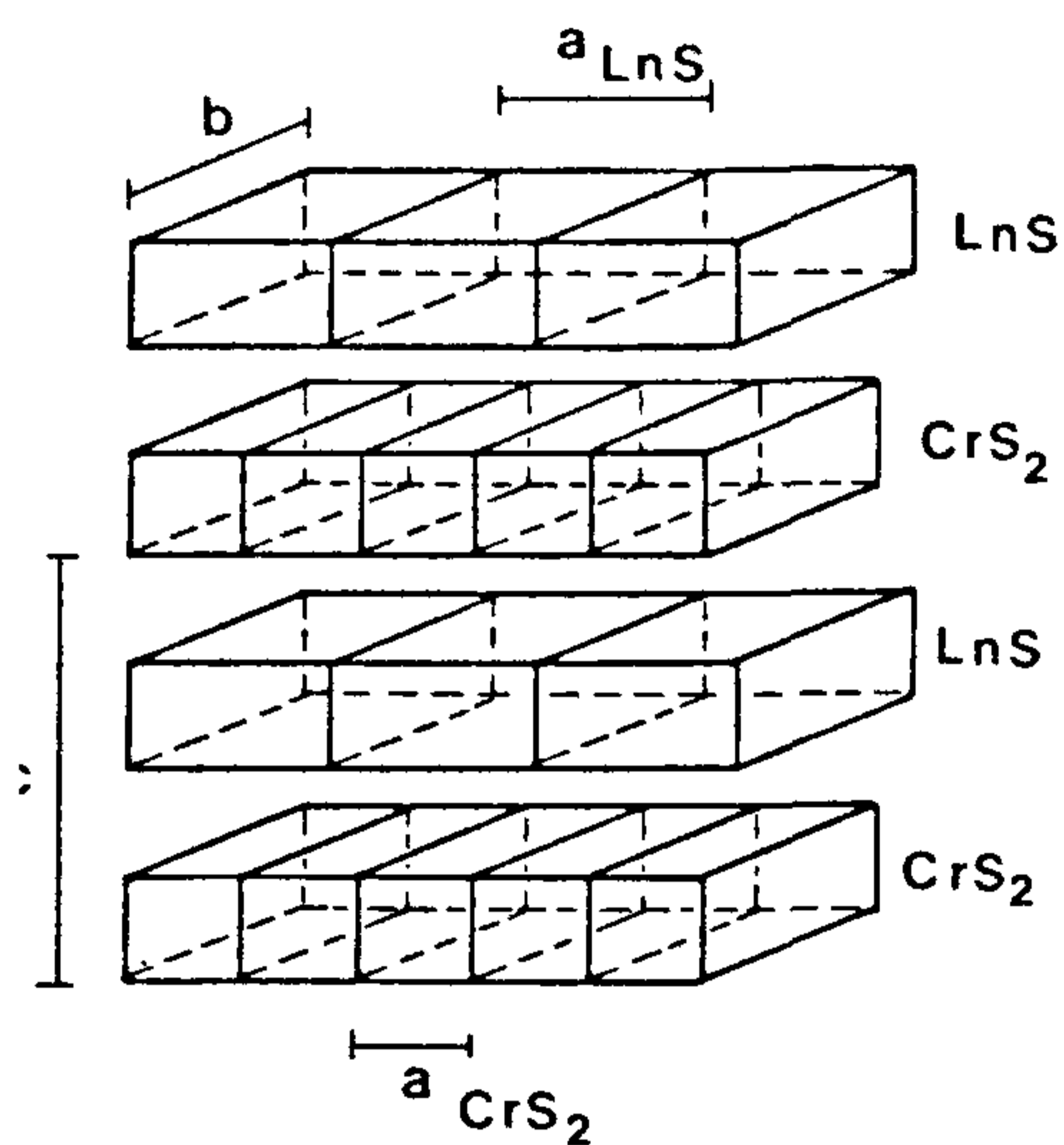
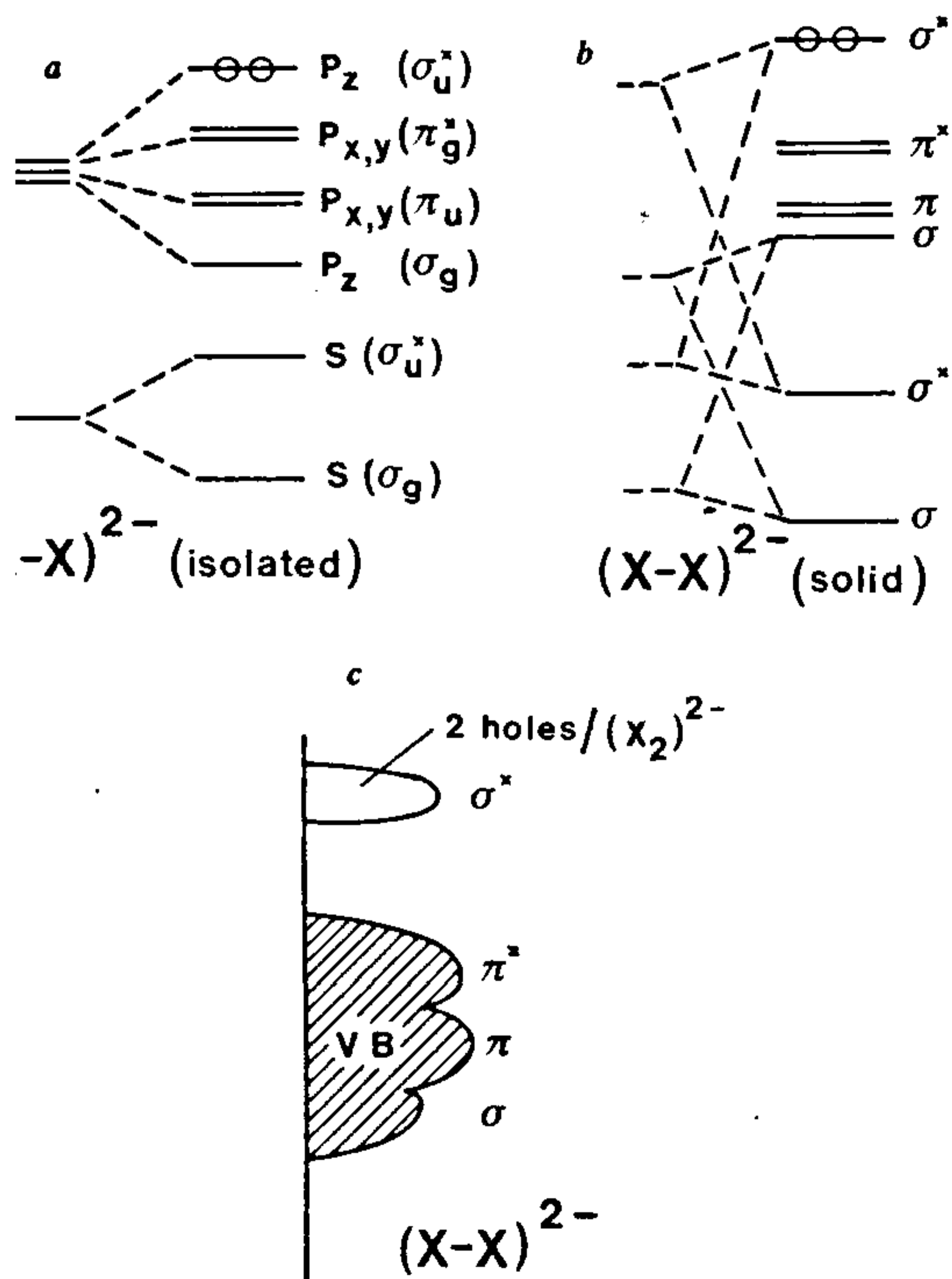


Figure 8. Condensation of three types of ribbons to build a slab in the $NbGe_xTe_2$ series of phases. Three examples: association abc in $MA_{1/3}Te_2$, 2a2bc association in $MA_{2/5}Te_2$, intermodulated compositions with $n(abc) + m(2a2bc)$.



9. $(\text{LnS})_{1+x}\text{CrS}_2$ misfit compounds show an alternation of (LnS) (pseudo NaCl) and CrS_2 ones (TiS_2 type). Incommensurability along a .



10. The formation of $(\text{X}_2)^{2-}$ ions (a) from s and p sulphur, leads in the solid to the sequence represented in (b) which in a broad sp band and a separated σ^* band (c).

pounds, the number of Ge atoms is equal to the number of Nb–Nb pairs. It could therefore be supposed that the two electrons donated by Ge are used by two Nb to form $(\text{Nb}^{3+})_2$ pairs. The other Nb atoms would be reduced through the transfer of electrons from the sp band. There is, however, no direct proof that such a hypothesis is correct. The interest in Ge_xNbTe_2 in the context of this contribution arises because both extra atoms (Ge, Si) acting as donors and Te associations contribute to stabilize the structure.

The Ge_xNbTe_2 phases show a segregation of ribbons in a plane, that is, in a two-dimensional space. Misfit layered chalcogenides³⁰ represent a case of segregation of slabs in three-dimensional space. With general formulation $(\text{MX})_{1+x}\text{TX}_2$, where $M=\text{Ln, Sn, Pb, Bi, Sb}$; $T=\text{Ti, V, Cr, Nb, Ta}$; $X=\text{S, Se}$; $0.08 < x < 0.28$, they present a structure which results from an alternate stacking of MX and TX_2 slabs (Figure 9). The MX slab is a double slice along 100 of a distorted NaCl arrangement. The TX_2 slabs are built up from sharing edges $[\text{TX}_6]$ octahedra ($T=\text{Ti, V, Cr}$) or trigonal prisms (Nb, Ta) like in TiS_2 or NbS_2 . The regular alternation of slabs gives a common c parameter for the two sublattices in the stacking direction. Each of these sublattices has two in-plane a and b parameters. So far the b parameters have been found to be identical. But the ratio of the a parameters is given by an irrational number, thus the misfit which is illustrated by the $1+x$ value in the chemical formulation. Again we find here systems with CrS_2 slabs. However they form only in case of LnS type MX slabs. Indeed these slabs behave as electron donors. Like rare earth monochalcogenides they can be represented by $\text{Ln}^{3+}\text{e}^-\text{S}^{2-}$ with one electron delocalized in $5d$ or $4f$ bands. It is this electron which is transferred to the CrS_2 slab, refilling the top of the sp band. The CrS_2 misfit compounds are infinite two-dimensional intercalation compounds. LnS layers play the same role as Na layers in NaCrS_2 . Sn/Pb S slabs which do not transfer any electrons do not lead to misfit phases with CrS_2 . In addition, the stoichiometry of the LnS slab is governed by the electron transfer. Exactly one electron is transferred. Vacancies are observed in the Ln^{3+} site. $(\text{GdS})_{1.27}\text{CrS}_2$, for example, is in fact $(\text{Gd}_{0.91}\square_{0.09}\text{S})_{1.27}\text{CrS}_2$ which corresponds to an exact charge balance between Gd^{3+} , Cr^{3+} and S^{2-} (ref. 31).

Conclusion

What has been described here is a chemistry of holes, a chemistry of antibonding states. Instead of populating the lowest energy levels with electrons, one is depopulating the top of a sp anionic band. The holes can associate leading to an anionic catenation which results in a cut off to the top of the sp band, as illustrated by the formation of the σ^* branch of the pyrite band

structure (Figure 10). Such an evolution takes place on the right part of the periodic table where the d–sp redox competition is most active. On the left part of it, the depletion of anionic levels results in an extra population of d cationic orbitals. There, the transferred electrons take part in the cationic clusterization that may be observed. The anionic associations driven by holes and the cationic association driven by electrons formally stand symmetrically on the right and left part of periodic table. The depopulation of anion antibonding states of course results in a shortening of the anion–anion distance. This change in anion–anion separation is simply related to the formal charge on anions and can even be taken as an indication of the amount of transferred electrons in an intercalation process when anionic pairs, for example, are taking them.

The control of the hole population at the top of a sp band leads to a very rich chimie douce of the redox type. The stability of compounds that may be formed through a deintercalation process essentially depends on the energy level at which holes will be introduced (CrS₂ and CrSe₂ cases). Neutralizing holes at the top of a sp band allows the stabilization of structural types that would not exist otherwise. These concepts open large avenues for new chemical synthesis. The physical properties have not been discussed here. If delocalized holes introduce a p type component in conductivity, they may also induce strong ferromagnetic coupling depending on structural geometry and electronic population of the cations (CuCr₂S₄ is a spectacular example). Finally, the role of holes in superconductivity as discussed by different groups and particularly by C. N. R. Rao in cuprates³², is also active in sulphide and selenides (copper chalcogenides provide good examples).

1. Meerschaut, A. and Rouxel, J., *J. Less Common Met.*, 1975, **39**, 197.
2. Hodeau, J. L., Marezzio, M., Roucau, C., Ayroles, R., Meerschaut, A., Rouxel, J. and Monceau, P., *J. Phys. C: Solid State Phys.*, 1978, **11**, 4117.
3. Haen, P., Monceau, P., Tissier, B., Waysand, G., Meerschaut, A., Molinié, P. and Rouxel, J., Proceedings of 14th International Conference on Low Temperature Physics, Otaniemi, Finland, 1975, vol. 5, pp. 445.
4. Chaussy, J., Haen, P., Lasjaunias, J. L. *et al.*, *Solid State Commun.*, 1976, **20**, 757.
5. Monceau, P., Ong, N. P., Portis, A. M., Meerschaut, A. and Rouxel, J., *Phys. Rev. Lett.*, 1976, **37**, 602.
6. Jellinek, F., in *Inorganic Sulfur Chemistry* (ed. Nickless, G.), Elsevier, Amsterdam, 1968.
7. Goodenough, J. B., *J. Phys. Chem. Solids*, 1969, **30**, 261.
8. Canadell, E., Jobic, S., Brec, R., Rouxel, J. and Whangbo, M. H., *J. Solid State Chem.*, 1992, **99**, 189.
9. Folmer, J. C. W., Jellinek, F. and Colis, J. H. M., *J. Solid State Chem.*, 1988, **72**, 137.
10. Klepp, K. O. and Ipsier, H., *Angew. Chem. Int. Ed. Engl.*, 1982, **21**, 911.
11. Canadell, E., Jobic, S., Brec, R. and Rouxel, J., *J. Solid State Chem.*, 1992, **98**, 70.
12. Jobic, S., Brec, R. and Rouxel, J., *J. Alloys Compounds*, 1992, **178**, 353.
13. Daoudi, A., Thesis Rennes, U., 1996 and Noel H. and Daoudi, A., to be published.
14. Rao, C. N. R. *et al.*, *Surface Sci.*, 1986, **177**, L971; also *Rev. Solid State Sci.*, 1990, **4**, 843.
15. Johrendt, D., Felser, C. and Rouxel, J., *J. Solid State Chem.*, 1997, in press.
16. Schöllhorn, R., *Angew. Chem. Int. Ed. Engl.*, 1988, **27**, 1392.
17. Van Bruggen, C. F., Haange, R. J., Wieggers, G. A. and de Boer, D. K. G., *Physica*, 1980, **B99**, 166.
18. Schöllhorn, R. and Payer, A., *Angew. Chem. Int. Ed. Engl.*, 1985, **24**, 67.
19. Murphy, D. and Sinha, S., *Solid State Ionics*, 1986, **20**, 81.
20. Berger, R. and Bucur, R. V., *Mater. Res. Bull.*, 1992, **27**, 439.
21. Berger, R., *J. Less Common Mat.*, 1989, **147**, 141.
22. Berger, R. and Van Bruggen, C. F., *J. Less Common Mat.*, 1984, **99**, 113.
23. Blandeau, L., Ouvrard, G., Calage, Y., Brec, R. and Rouxel, J., *J. Phys. C.*, 1987, **20**, 4271.
24. Ouvrard, G., Freour, R., Brec, R. and Rouxel, J., *Mat. Res. Bull.*, 1985, **20**, 1985.
25. Jandali, M. Z., Enlenberger, G. and Hahn, H., *Z. Anorg. Allg. Chem.*, 1980, **470**, 39.
26. Iglesias, J. E., Pachali, K. E. and Steinfink, H., *Mat. Res. Bull.*, 1972, **7**, 1247.
27. Zhang, X., Hogan, T., Kannewurf, C. R. and Kanatzidis, M. G., *J. Alloys Compounds*, 1997, in press.
28. Ouvrard, G., Brec, R. and Rouxel, J., Unpublished results and *Ann. Chim. Paris*, 1982, **7**, 53.
29. a) Monconduit, L., Evian, M., Boucher, F., Brec, R. and Rouxel, J., *Anorg. Allg. Chem.*, 1992, **616**, 177; b) Li, J., Badding, E. and DiSalvo, F. J., *J. Alloys Compounds*, 1992, **184**, 257; c) Van der Lee, A., Evain, M., Monconduit, L., Brec, R. and Petricek, V., *Inorg. Chem.*, 1994, **33**, 3032; d) Rouxel, J. and Evain, M., *Eur. J. Solid State Inorg. Chem.*, 1994, **31**, 683.
30. For a general description see: a) Rouxel, J., Meerschaut, A. and Wieggers, G., *J. Alloys Compounds*, 1995, **229**, 144–157; b) Wieggers, G., Meerschaut, A., in *Incommensurate Sandwiched Layered Compounds* (ed. Meerschaut, A.), Trans. Tech. Publications, 1992, pp. 104–172.
31. Rouxel, J., Moïlo, Y., Lafond, A., DiSalvo, F. J., Meerschaut, A. and Roesky, R., *Inorg. Chem.*, 1994, **33**, 3358.
32. Rao, C. N. R., *Chem. Soc. Rev.*, 1995, **24**, 1.

Received 31 May 1997; accepted 2 June 1997